

## Photodegradation of methylene blue with a titanium dioxide/polyacrylamide photocatalyst under sunlight

Foad Kazemi, Zahra Mohamadnia, Babak Kaboudin, Zeinab Karimi

Department of Chemistry, Institute for Advanced Studies in Basic Sciences, Gava Zang, P. O. Box 45195-1159, Zanjan, Iran  
Correspondence to: F. Kazemi (E-mail: kazemi\_f@iasbs.ac.ir) and Z. Mohamadnia (E-mail: z.mohamadnia@iasbs.ac.ir)

**ABSTRACT:** Hydrogels containing TiO<sub>2</sub> nanoparticles (NPs) have photocatalytic properties and degrade pollutants under light. In this study, a polyacrylamide (PAAm) hydrogel was synthesized with TiO<sub>2</sub> P25 NPs as the initiator, acrylamide as a monomer, and *N,N'*-methylene bisacrylamide as a crosslinker in aqueous media under sunlight. Fourier transform infrared spectroscopy, thermogravimetric analysis, scanning electron microscopy, and transmission electron microscopy were applied to characterize the TiO<sub>2</sub>/PAAm hydrogel. The effects of different synthetic conditions, such as the initiator concentration, crosslinker, and dilution, on swelling were investigated. The maximum swelling of the TiO<sub>2</sub>/PAAm hydrogel was 45 g/g in the hydrogel synthesized with optimum conditions by 0.2% TiO<sub>2</sub>. The photocatalytic degradability of the hydrogel was investigated with methylene blue (MB) as the pollutant target. Also, the effects of the pH and MB concentration were studied. Under optimum conditions, 95.00% of the MB was degraded by the TiO<sub>2</sub>/PAAm photocatalyst after 5 h of irradiation under sunlight. The comparison of the results with those of the TiO<sub>2</sub> P25 powder showed that the TiO<sub>2</sub> NPs had better activity than the hydrogel, but unlike the hydrogel, the activity of these NPs decreased in each recycling time because of the aggregation of NPs. Finally, the hydrogel was recycled seven times without a considerable reduction in the degradation efficiency. © 2016 Wiley Periodicals, Inc. *J. Appl. Polym. Sci.* **2016**, *133*, 43386.

**KEYWORDS:** crosslinking; hydrophilic polymers; photopolymerization; properties and characterization; swelling

Received 5 October 2015; accepted 28 December 2015

DOI: 10.1002/app.43386

### INTRODUCTION

A semiconductor is a material whose electrical conductivity and band gap are between those of conductive and nonconductive materials.<sup>1</sup> One of the major applications of these materials is in photocatalytic reactions; these materials include alkanes, halo alkanes, aliphatic alcohols, carboxylic acids, alkenes, aromatics, halo aromatics, polymers, surfactants, herbicides, pesticides, and dyes.<sup>2</sup> In recent years, the rapid growth of industry and the high use of chemical pollutants have caused water pollution. Dyes are one of these pollutants, and they are used extensively in the textile, paper, plastics, cosmetic, and food industries.<sup>3</sup> About 10–15% of dyes enter wastewater during the coloring process, and these cause serious ecological problems. So, the removal of contaminants from wastewaters and their degradation is important.<sup>4</sup>

Methylene blue (MB) is a heterocyclic aromatic chemical compound that applies in different fields, such as biology and chemistry.

It has a characteristic deep blue color in the oxidized state, but the reduced form, leucomethylene blue (LMB), is colorless (Figure 1).<sup>5</sup>

Conventional methods for dye removal from industrial wastewaters include biological treatment, coagulation, flotation, electrochemical techniques, adsorption, and oxidation.<sup>6</sup> These methods need many steps and processes, and they usually convert pollutants from one form to another (e.g., from the liquid state to the solid state). So, new methods with a greater efficiency and lower energy must be developed.<sup>7</sup> In recent years, advanced oxidation processes that break pollutants down into biodegradable products have been used in wastewater treatment.<sup>8</sup> Advanced oxidation processes are based on the production of reactive hydroxyl radicals that attack pollutant molecules rapidly without selectivity and degrade them.<sup>7</sup> Hydroxyl radicals can be produced by chemical, photochemical, and photocatalytic methods.<sup>9</sup> For example, in one photocatalytic method, semiconductor nanoparticles (NPs), such as TiO<sub>2</sub> NPs as a heterogeneous photocatalyst, and a light source are applied to excite valence-band electrons.<sup>10</sup> The advantages of TiO<sub>2</sub> NPs include their strong oxidation power, nontoxicity, long-term photostability, and activity in the visible region.<sup>11,12</sup> TiO<sub>2</sub> P25 is a commercial form of TiO<sub>2</sub> NPs, and its crystalline structure contains 80% anatase and 20% rutile phases. When TiO<sub>2</sub> is illuminated with a wavelength below 380 nm, the electrons from

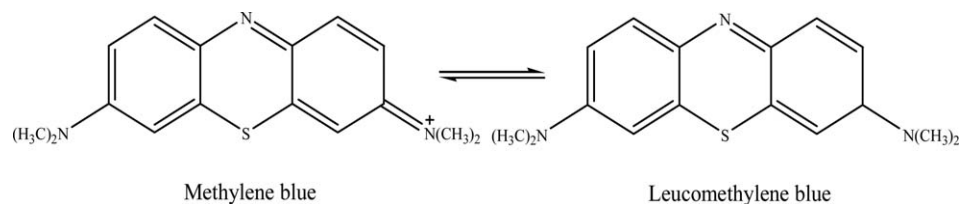


Figure 1. Structures of MB and LMB.<sup>5</sup>

the valence band excite through the band gap into the conduction band and leave holes in the valence band. Then, the holes react with water molecules or hydroxyl ions ( $\text{OH}^-$ ) and produce hydroxyl radicals. Hydroxyl radicals are very strong oxidants that degrade pollutants.<sup>9</sup>

In practice,  $\text{TiO}_2$  NPs (and other semiconductors) are used in a powdery form, and their separation and recycling from treatment water after dye degradation is a problem.<sup>13,14</sup> To overcome this problem,  $\text{TiO}_2$  NPs can be loaded in different matrixes, including polymers.<sup>15–18</sup> Hydrogels are three-dimensional networks of hydrophilic polymers that can swell in water and hold a large amount of water while maintaining their structure.<sup>19</sup> The advantages of the application of  $\text{TiO}_2$  in the hydrogel matrix are its low cost and easy recycling and the prevention of the recombination of electron holes.<sup>15</sup> These materials can be produced with several polymerization methods from vinyl monomers. The polymerization of vinyl monomers can be initiated with semiconductor NPs by UV irradiation; this is called *photopolymerization*.<sup>20</sup> Photopolymerization has many advantages, including the fact that it is a mild and easy process, but the direct use of available sunlight as a light source in the polymerization of vinyl monomers is still a challenge because the intensity of sunlight is partially diluted.<sup>21</sup> Photoinitiators, such as  $\text{TiO}_2$ , CdTe, and ZnO NPs, have been applied to the polymerization of vinyl monomers.<sup>22</sup> There have been several reports in which semiconductors were applied to the polymerization of vinyl monomers under UV light.<sup>23–25</sup> Zhang *et al.*<sup>21</sup> reported the polymerization of *N,N*-dimethyl acrylamide using semiconductor NPs as the initiator under sunlight. Also, Bao *et al.*<sup>26</sup> carried out the polymerization of *N,N*-dimethyl acrylamide and 2-acrylamide-2-methyl propane sulfonic acid monomers with a 2,2-diethoxyacetophenone photoinitiator. Then, this hydrogel was applied to the adsorption and, after that, the photodegradation of MB.

Hydrogels prepared with semiconductor NPs have photocatalytic activity and, so, can be applied to the degradation of pollutants from wastewaters.

In this study, a novel  $\text{TiO}_2$ /polyacrylamide (PAAm) photocatalyst was synthesized by aqueous solution polymerization. Then, its ability to remove MB as a pollutant from an aqueous solution was evaluated. Ninety-five percent of MB was degraded during 5 h after irradiation by sunlight. This hydrogel was recovered seven times.

## EXPERIMENTAL

### Materials

An acrylamide (AAM) monomer was commercially purchased from Daejung Co. *N,N'*-Methylene bisacrylamide (MBA) was

obtained from Merck Co.  $\text{TiO}_2$  P25 (containing 20% rutile and 80% anatase phases with an elementary particle size of 34 nm and a Brunauer–Emmett–Teller surface area of about  $70 \text{ m}^2/\text{g}$ ) was purchased from Degussa Corp. and was used as the photoinitiator. MB was purchased from Merck Co. and was used as the pollutant model. All chemicals were used as received without further purification.

### Characterization

IR spectroscopy was carried out on a Bruker Vector 22 Fourier transform infrared (FTIR) spectrometer (Germany) in the region  $4000\text{--}500 \text{ cm}^{-1}$ . The samples were prepared in the form of pellets with KBr under ambient conditions and were measured in transmission mode. The adsorption ultraviolet–visible (UV–vis) spectra of the samples were obtained with an Ultrospec 3100 pro spectrophotometer. The thermal analysis of the sample was performed with a Netzsch STA 409 PC 141H Luxx instrument (Germany) at a heating rate of 20 K/min under an  $\text{N}_2$  atmosphere in a temperature range from 25 to 900 °C. Before analysis, the  $\text{TiO}_2$ /PAAm photocatalyst was dried at 60 °C for about 24 h in an oven and then ground. Scanning electron microscopy (SEM) micrographs of the samples were obtained with a Hitachi S-4160 field emission–SEM microscope. Transmission electron microscopy (TEM) images were recorded with a cm120 model instrument (Philips Co., The Netherlands).

### Preparation of the PAAm Hydrogel with a $\text{TiO}_2$ P25 Initiator ( $\text{TiO}_2$ /PAAm)

An amount of 0.3 g of AAM was dissolved in 6 mL<sup>21</sup> of distilled water in a 50-mL round-bottomed balloon. Then, 0.0037 g of MBA (MBA/AAM = 1:80)<sup>27</sup> was added to the monomer solution under stirring. After MBA was dissolved, 0.12 mL of a  $\text{TiO}_2$  aqueous suspension (1% w/v)<sup>21</sup> was added to the mixture. This mixture was sonicated for 5 min to better disperse the  $\text{TiO}_2$  NPs. Finally, the mixture was placed under sunlight irradiation. After gel formation, the mixture was washed several times with distilled water to remove unreacted materials and then dried at 60 °C in an oven.

### Swelling Behavior of the Hydrogels

A gravimetric procedure was used to monitor the swelling behavior of the composite hydrogels in deionized water. Briefly, a known mass of the hydrogel (0.1 g) was immersed in 100 mL of deionized water at room temperature to achieve equilibrium swelling. The swollen samples were then separated from unabsorbed water by filtration. The water absorbency was calculated as follows:

$$S = \frac{W - W_0}{W_0}$$

where  $S$  is amount of swelling,  $W$  is the weight of the swollen hydrogel, and  $W_0$  is the weight of the dry sample. In this section, each experiment was repeated two times.

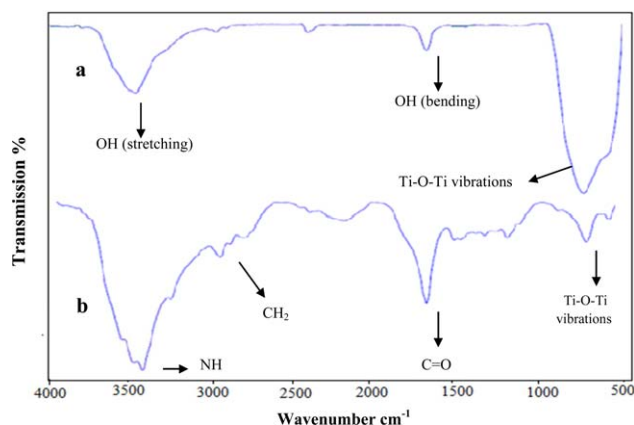


**Figure 2.** FTIR spectra of the (a)  $\text{TiO}_2$  P25 NPs and (b)  $\text{TiO}_2/\text{PAAM}$  hydrogel. [Color figure can be viewed in the online issue, which is available at [wileyonlinelibrary.com](http://wileyonlinelibrary.com).]

### Photocatalytic Experiments<sup>28</sup>

The photocatalytic activity and degradability of the  $\text{TiO}_2/\text{PAAM}$  hydrogel were investigated with MB as an effluent model. For this purpose, 0.2 g of  $\text{TiO}_2/\text{PAAM}$  was added to 25 mL of a 10-ppm MB solution. The photocatalytic degradation experiment was carried out in open air under sunlight. At indicated time intervals, 3 mL of dye solution was removed, the concentration of dye was measured with UV-vis spectroscopy, and the degradation percentage ( $D$ ) of the MB solution was calculated with the following formula:

$$D = \frac{A_0 - A_1}{A_0} \times 100 = \frac{C_0 - C_1}{C_0} \times 100 \quad (1)$$

where  $A_0$ ,  $A$ ,  $C_0$ , and  $C$  are the absorbances and concentrations of the MB solution at a maximum absorption peak ( $\lambda_{\text{max}}$ ) of 665 nm before and after irradiation, respectively.

### Decolorization of the Dye Solution in the Dark<sup>28</sup>

To confirm the effect of light on the dye degradation, 0.2 g of the  $\text{TiO}_2/\text{PAAM}$  photocatalyst was added to 25 mL of a 10-ppm MB solution and placed in the dark. Then, at different time intervals, the dye removal was investigated.

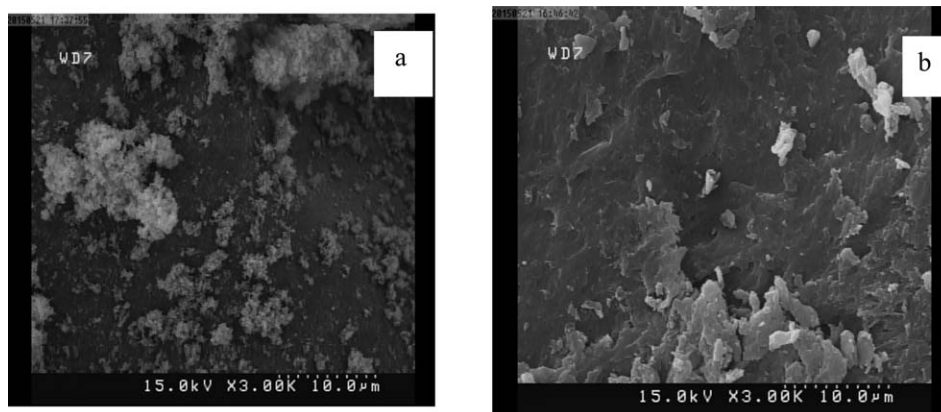


**Figure 3.** SEM images of the (a)  $\text{TiO}_2$  P25 NPs and (b)  $\text{TiO}_2/\text{PAAM}$  hydrogel.

### Degradation of the Dye by Powdery $\text{TiO}_2$ P25

The photodegradation of MB by  $\text{TiO}_2$  P25 powder was also studied. The reaction mixture was prepared the addition of 0.006 g of  $\text{TiO}_2$  powder (equal to the amount of  $\text{TiO}_2$  used in the hydrogel synthesis) to 25 mL of a MB solution (10 mg/L). The suspension was sonicated for 5 min and stirred magnetically for 20 min without light to reach equilibrium adsorption between MB and the  $\text{TiO}_2$  nanostructures.<sup>14</sup> The degradation process was followed by UV-vis spectroscopy.

## RESULTS AND DISCUSSION

### Characterization

**FTIR Spectroscopy.** In the  $\text{TiO}_2$  P25 spectrum [Figure 2(a)], the absorption peaks at 3417 and 1627  $\text{cm}^{-1}$  were attributed to  $-\text{OH}$  stretching and bending vibrations, and that at 664  $\text{cm}^{-1}$  belonged to  $\text{Ti}-\text{O}-\text{Ti}$  vibrations. In the  $\text{TiO}_2/\text{PAAM}$  spectrum [Figure 2(b)], the absorption peak at 3416  $\text{cm}^{-1}$  was attributed to  $\text{OH}$  stretching vibrations, that at 1626  $\text{cm}^{-1}$  belonged to  $\text{C}=\text{O}$  stretching vibrations, that at 2928  $\text{cm}^{-1}$  was due to  $-\text{CH}_2-$  stretching vibrations, that at 1451  $\text{cm}^{-1}$  was due to  $\text{C}-\text{N}$  stretching vibrations, that at 1119  $\text{cm}^{-1}$  was due to  $\text{C}-\text{O}$  stretching vibration, and that at 622  $\text{cm}^{-1}$  belonged to  $\text{Ti}-\text{O}-\text{Ti}$  vibrations.

**SEM.** The morphologies of  $\text{TiO}_2$  P25 and the  $\text{TiO}_2/\text{PAAM}$  (0.5% w/v  $\text{TiO}_2$ ) photocatalyst are shown in Figure 3. As shown, the  $\text{TiO}_2$  P25 particles were small spherical particles, but they had a tendency to agglomerate together. The  $\text{TiO}_2/\text{PAAM}$ , which was obtained from photopolymerization in an aqueous solution, was basically a rough sheet, and this confirmed the presence of  $\text{TiO}_2$  NPs with a significant particulate nature.

**TEM.** TEM images of  $\text{TiO}_2$  P25 and the  $\text{TiO}_2/\text{PAAM}$  (0.5% w/v  $\text{TiO}_2$ ) photocatalyst are shown in Figure 4. TEM analysis revealed that the  $\text{TiO}_2$  NPs, with sizes of approximately 40 nm, were dispersed in the gel, and little accumulation was observed. So, we concluded that the initial size of the  $\text{TiO}_2$  NPs was preserved in the hydrogel.

**Thermogravimetric Analysis (TGA).** The TGA curve of the  $\text{TiO}_2/\text{PAAM}$  photocatalyst is shown in Figure 5. TGA of  $\text{TiO}_2/\text{PAAM}$  showed four weight losses at various temperatures. The first weight loss, in the range 25–200  $^{\circ}\text{C}$ , was attributed to the

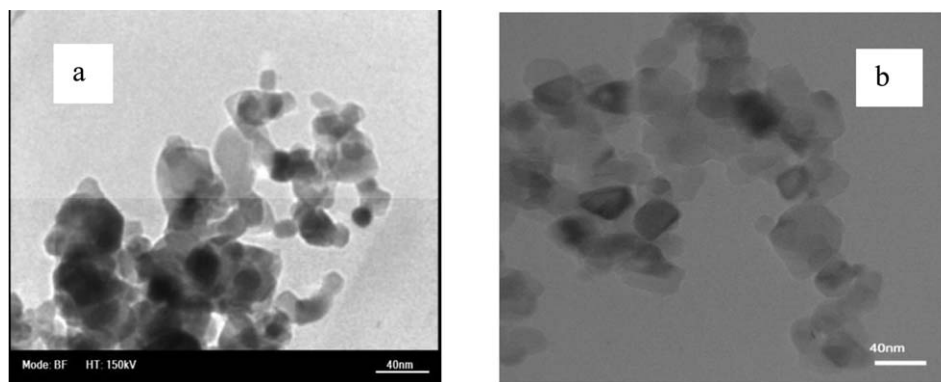


**Figure 4.** TEM images of the (a)  $\text{TiO}_2$  P25 NPs and (b)  $\text{TiO}_2$ /PAAm hydrogel.

evaporation of water molecules. According to the available band energies (Table I), the second weight loss was attributed to the breaking of C—N bonds in amide side groups and MBA moieties in the network because of the lower bond energy, which caused the evacuation of ammonia gas. Accordingly, the third and fourth weight losses, in the ranges 340–470 and 470–860 °C, respectively, were related to the breakage of polymer chains, which occurred at higher temperatures. Finally, the residual mass (9.13%) was attributed to the  $\text{TiO}_2$  NPs because of the high thermal stability.

#### Investigation the Effects of Different Synthetic Conditions on the Swelling Behavior of the Hydrogels

The swelling of synthesized hydrogels with different concentrations of  $\text{TiO}_2$  NPs (0.2, 0.5, 1.0, and 2.0% w/v) and different amounts of crosslinker and solvent were investigated. As shown in Figure 6(a), the swelling of the hydrogel decreased when the  $\text{TiO}_2$  concentration was increased because the higher concentration of  $\text{TiO}_2$  led to an increase in the strength of the hydrogel network and a reduction in the absorbance capacity.

It has been proven that the concentration of the crosslinker affects the swelling and mechanical properties of the hydrogel.<sup>29</sup> So, hydrogels with different concentrations of MBA as the crosslinker (0, 1:160, 1:80, and 1:40) were synthesized. As shown in Figure 6(b), the swelling of the hydrogels decreased with increasing crosslinker concentration. Generally, low concentrations of crosslinker lead to a lower crosslinking density and higher swelling capacity, whereas a gel formed with a high crosslinker concentration will possess a higher crosslinking density. This causes a decrease in the distance between the crosslinking points and, thereby, lowers the swelling capacity.<sup>30</sup>

In general, the size of the pores of the synthesized hydrogel can be controlled by careful adjustment of various factors, such as the types and amounts of surfactant, porogens, and gas-forming agent during polymerization and the amount of diluent (usually water) in the monomer mixture (i.e., the monomer/diluent ratio).<sup>31</sup> To investigate the effect of the monomer matrix dilution, the swelling of a hydrogel synthesized with 12 mL of distilled water was compared with the swelling of a hydrogel synthesized with 6 mL of distilled water. The swelling values

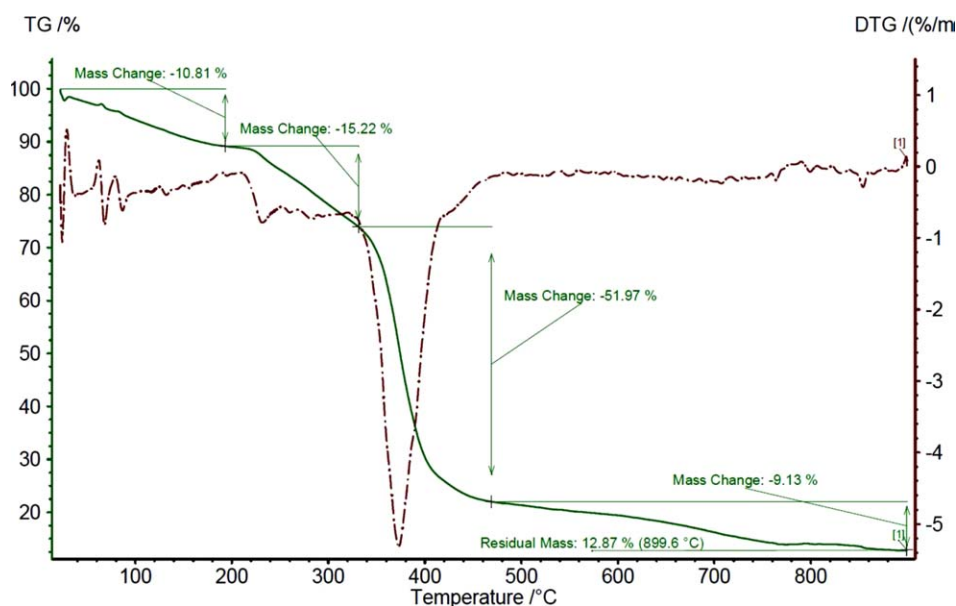


**Figure 5.** TGA curve of the  $\text{TiO}_2$ /PAAm (TG = thermogravimetry; DTG = derivative thermogravimetry). [Color figure can be viewed in the online issue, which is available at [wileyonlinelibrary.com](http://wileyonlinelibrary.com).]

**Table I.** Average Energies for the PAAm Bond Types<sup>15</sup>

Type of bond	Energy (kJ/mol)
C—N	305
C—C	347
N—H	391
C—H	413
C=O	745

were 42 versus 26 g/g for the hydrogels synthesized with 12 and 6 mL, respectively, of diluent (distilled water); this confirmed the positive effect of dilution on the swelling of the hydrogels.

Because of the positive effect of dilution on the hydrogel swelling, this effect was also investigated for hydrogels with different amounts of TiO<sub>2</sub> NPs (0.5, 1.0, and 2.0% w/v TiO<sub>2</sub>). Figure 6(c) shows the swelling of the diluted hydrogels in deionized water. A comparison between Figures 6(a) and 6(c) showed the positive effects of dilution on the water absorbance capacity and swelling.

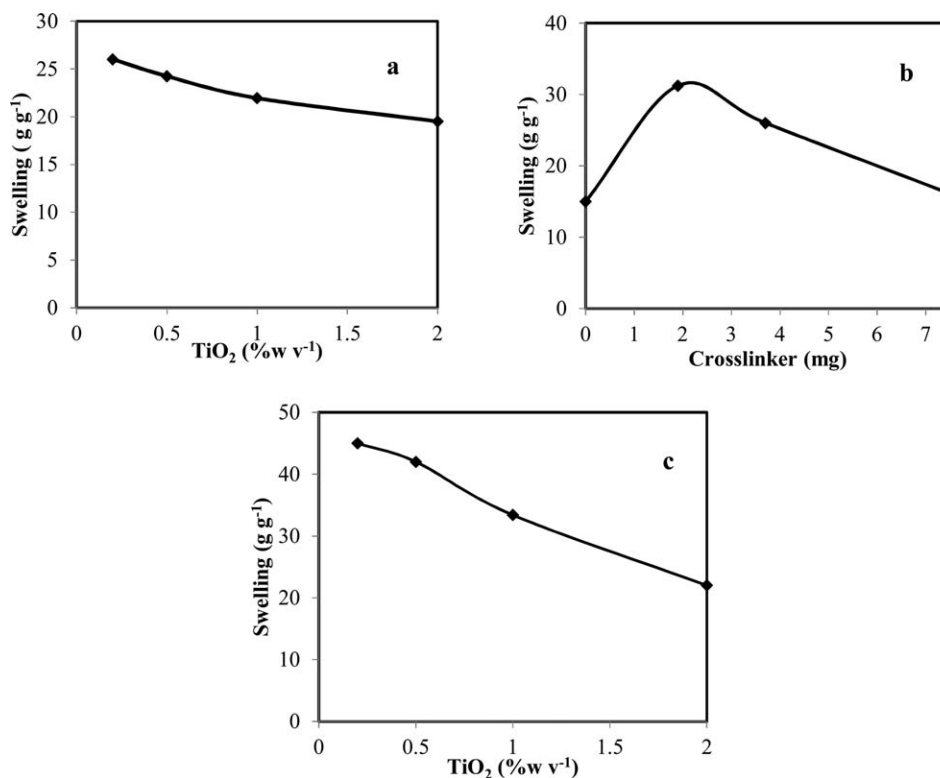
#### Investigation the Effect of the Hydrogel Synthesis Conditions on the MB Photodegradation

The effects of different synthetic conditions of the hydrogels on MB photodegradation were investigated. Figure 7(a) shows the degradation efficiency of MB with 0.2-g hydrogels containing different concentrations of TiO<sub>2</sub> P25 at different time intervals. The

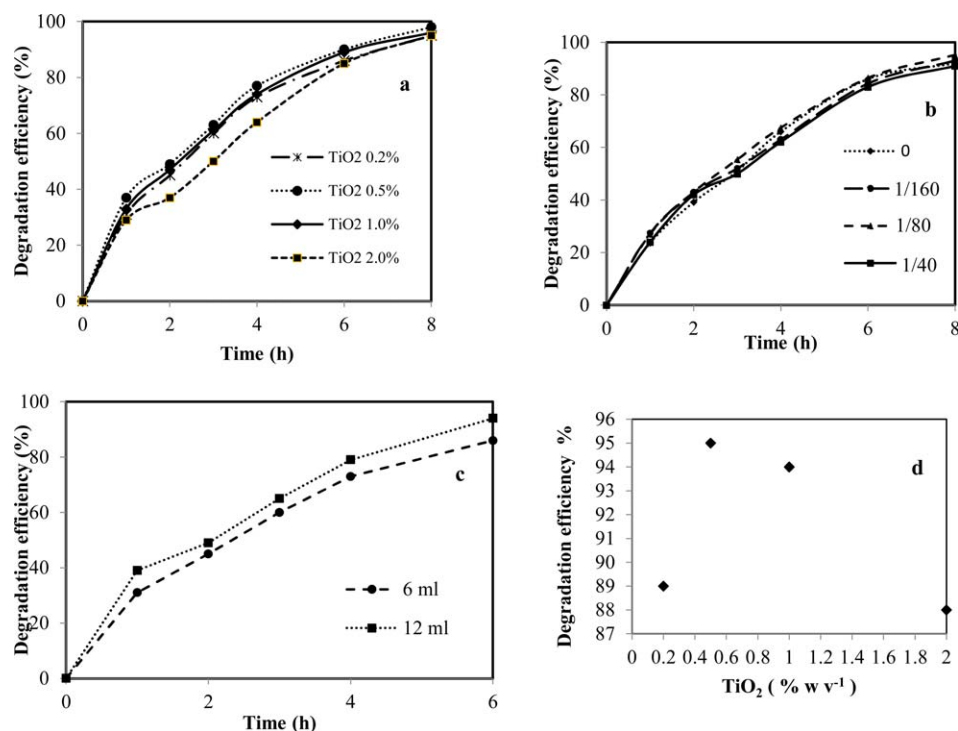
rate of MB degradation with these hydrogels was approximately similar, but in the case of the 2.0% w/v TiO<sub>2</sub> degradation at the first time interval, the MB degradation was lower than those of the other TiO<sub>2</sub> concentrations; this may have been related to the aggregation of TiO<sub>2</sub> nanoparticles (NPs) at higher concentrations of TiO<sub>2</sub> P25.<sup>32</sup> However, after 8 h, all of the TiO<sub>2</sub> concentrations degraded approximately equal amounts of MB. The results were very close together, and the TiO<sub>2</sub> P25 concentration had no effect on the MB degradation. So, at this stage, the minimum concentration of TiO<sub>2</sub> (0.2% w/v) was selected as the optimum condition because of its cost effectiveness.

Figure 7(b) shows the degradation efficiency of MB with hydrogels with different concentrations of MBA crosslinker. As shown in Figure 7(b), the MBA concentration had approximately no significant effect on the MB degradation, and the small observed differences were probably due to the differences in the sunlight intensity on different days. We concluded that the removal of MB was not according to dye absorbance, but it was a photocatalytic reaction. The ratio of 1:80 was selected as the optimum MBA concentration because it had good mechanical strength toward the 1:160 ratio, a higher swelling toward the 1:40 ratio, and an easy recyclability toward hydrogels without crosslinker.

Then, the effect of the monomer matrix dilution on MB photodegradation was investigated. The results are shown in Figure 7(c). According to Figure 7(c), when the amount of diluent (distilled water here) in the monomer mixture increased, the



**Figure 6.** Effects of the synthetic conditions on the hydrogel swelling: (a) effect of the TiO<sub>2</sub> concentration (AAm = 0.3 g, MBA/AAm = 1:80, water = 6 mL), (b) effect of crosslinking (AAm = 0.3 g, TiO<sub>2</sub> 0.2% w/v = 0.12 mL, water = 6 mL), and (c) effect of the TiO<sub>2</sub> concentration in the diluted monomer matrix (AAm = 0.3 g, MBA/AAm = 1:80, water = 12 mL).



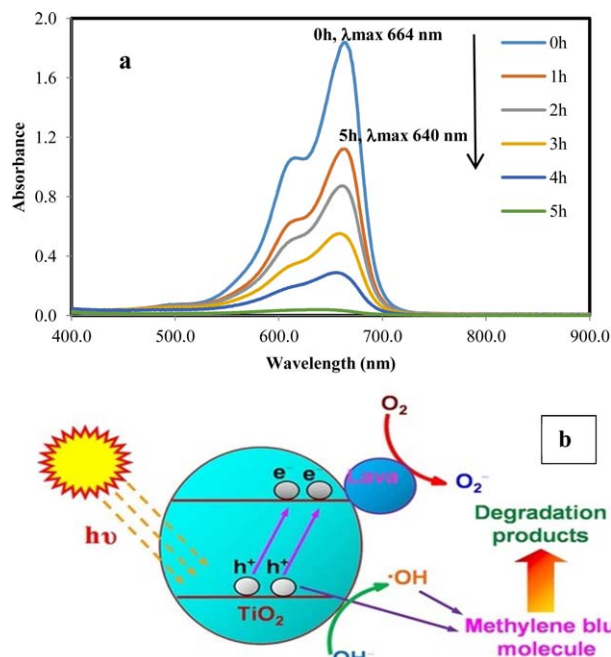
**Figure 7.** Effects of the synthetic conditions on the MB photodegradation (sunlight intensity =  $101 \times 103$ ): (a) TiO<sub>2</sub> P25 concentration, (b) crosslinker concentration, (c) dilution of the monomer matrix, and (d) simultaneous effect of the TiO<sub>2</sub> P25 concentration and monomer matrix dilution. [Color figure can be viewed in the online issue, which is available at [wileyonlinelibrary.com](http://wileyonlinelibrary.com).]

rate of MB degradation also increased because the pore size of the synthesized gel increased up to the micrometer range and light could easily diffuse into the hydrogel. This result was confirmed previously. Finally, according to the positive effect of dilution on swelling, this effect was also investigated for other concentrations of TiO<sub>2</sub> (0.5, 1.0, and 2.0% w/v). The results are shown in Figure 7(d). We observed that the MB degradation of the hydrogel synthesized with 0.5% w/v TiO<sub>2</sub> was greater than that of other samples; it was approximately similar to that of 1.0% w/v TiO<sub>2</sub>. In the case of 0.2% w/v TiO<sub>2</sub>, because of the low concentration of TiO<sub>2</sub> and hence the low production of OH radicals, the rate of MB degradation was low. At a high concentration of TiO<sub>2</sub> (2.0% w/v), three reasons can be given for the diminished rate of MB degradation:

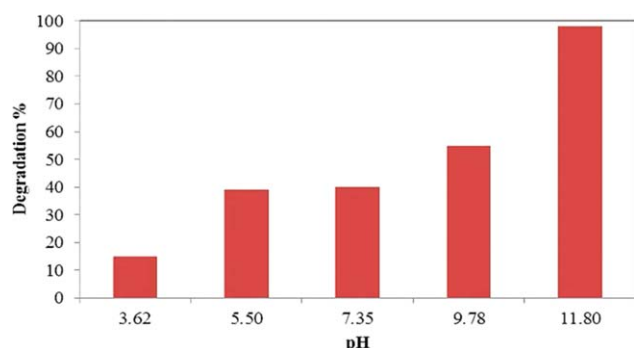
1. Hydrogels containing high quantities of TiO<sub>2</sub> showed low swelling, and so, the influence of MB molecules on the hydrogel decreased, and the scattering of light increased; this resulted in low degradation of the dye.
2. With large quantities of TiO<sub>2</sub> NPs, the pathway of light to reach MB molecules was hindered; this was probably due to light scattering at higher amounts of TiO<sub>2</sub> photocatalyst.<sup>32</sup>
3. At high concentrations of TiO<sub>2</sub> NPs, the aggregation and agglomeration of NPs reduced the active surface area of the catalyst and, thus, decreased the rate of MB degradation.<sup>33</sup> According to the mentioned reasons, 0.5 w/v % TiO<sub>2</sub> P25 was selected as the optimum amount.

Figure 8 shows the UV–vis spectra of the aqueous solution of MB in the presence of TiO<sub>2</sub>/PAAm. As shown in Figure 8(a),

$\lambda_{\max}$  in the visible region at 664 nm shifted to 640 nm after 5 h. This blueshift indicated that the demethylation of MB occurred at the catalyst (TiO<sub>2</sub>/PAAm) surface.<sup>34</sup> Figure 8(b)



**Figure 8.** (a) UV–vis spectra of the degradation of MB with the TiO<sub>2</sub>/PAAm photocatalyst as a function of the time and (b) schematic of MB degradation.  $h$ , planck constant;  $\nu$ , frequency of sunlight. [Color figure can be viewed in the online issue, which is available at [wileyonlinelibrary.com](http://wileyonlinelibrary.com).]



**Figure 9.** Effect of the MB solution pH on the photodegradation of MB at a constant irradiation time (1 h) under sunlight. [Color figure can be viewed in the online issue, which is available at [wileyonlinelibrary.com](http://wileyonlinelibrary.com).]

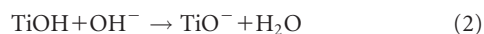
shows a schematic of MB photodegradation, which caused the exiting of the degradation products.<sup>35</sup>

#### Effect the pH of the MB Solution on the Degradation Efficiency

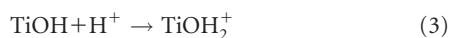
Other ions and contaminants can change the real pH of the effluent, so studying the effect of the pH on MB photodegradation was important.<sup>36</sup> The role of pH on MB photodegradation was investigated in the pH range 3.62–11.80 at a 10-ppm MB concentration and with 0.2 g of the TiO<sub>2</sub>/PAAm photocatalyst (synthesized by 0.5% w/v TiO<sub>2</sub> P25) with a constant irradiation time (1 h). Figure 9 shows the effect of pH on the MB degradation percentage after 1 h under sunlight.

The degradation efficiency in alkaline media increased. Three reasons for this phenomenon can be mentioned. The major reason for this phenomenon was due to the hydrolysis of amide groups in strong alkaline media; these groups were converted to carboxylate. In this state, the swelling of the hydrogel increased, and more MB molecules were absorbed by the hydrogel.

Furthermore, the increase in the rate of degradation in alkaline media could have been due to the change in the surface charge of TiO<sub>2</sub> and the ionization state of MB. The point of zero charge of TiO<sub>2</sub> was approximately 6.8.<sup>36</sup> At a pH of higher than 6.8, the surface of TiO<sub>2</sub> became negatively charged according to the following electrochemical reaction:



At a pH lower than the point of zero charge, the surface of TiO<sub>2</sub> was positively charged according to the following electrochemical reaction:



Because of the previous electrochemical equations and ionization state of MB, we calculated that in alkaline environments, there was a strong adsorption of MB on the TiO<sub>2</sub> particles as a result of the electrostatic interaction of the negatively charged TiO<sub>2</sub> with the cationic MB. In acidic media, TiO<sub>2</sub> is positively charged, and thus, there was a repulsive electrostatic force between TiO<sub>2</sub> and MB, which reduced the rate of degradation.<sup>36</sup>

The third reason for the increase in the rate of MB degradation in alkaline media was the facilitation of hydroxyl radical formation because of the high concentration of hydroxyl ions.<sup>37</sup>

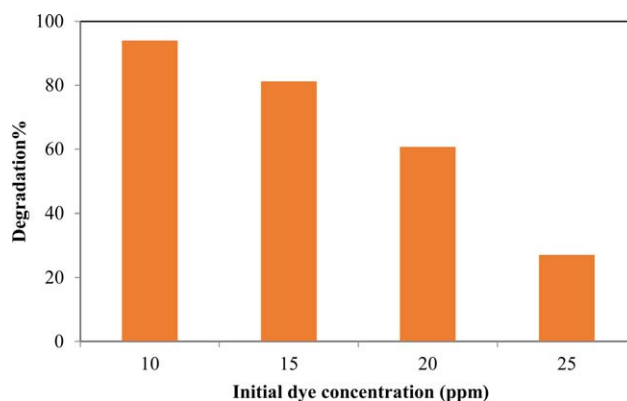


**Figure 10.** Effect of the initial MB concentration on the photocatalytic degradation at a constant irradiation time (5 h) under sunlight. [Color figure can be viewed in the online issue, which is available at [wileyonlinelibrary.com](http://wileyonlinelibrary.com).]

#### Effect of the Initial MB Concentration on the Degradation Efficiency

The effect of the initial dye concentration was studied by the variation of MB concentration from 10 to 25 ppm at a constant catalyst amount of 0.2 g TiO<sub>2</sub>/PAAm (0.5% w/v TiO<sub>2</sub>) for 5 h under sunlight. Figure 10 shows that the degradation percentage of dye decreased with its increasing concentration. Because at a high concentration of MB, the number of dye molecules absorbed on the catalyst surface increased.<sup>38</sup> Also, the high concentration reduced the production of hydroxyl radicals (OH<sup>•</sup>) by reducing solar light irradiation on the photocatalyst particles; finally, it caused the lower efficiency of MB degradation.<sup>39</sup>

#### Effect of the Hydrogel Matrix on the TiO<sub>2</sub> Activity

To investigate the effect of the hydrogel matrix on TiO<sub>2</sub> activity, MB photodegradation (10 ppm) was carried out by TiO<sub>2</sub> P25 powder (6 mg). The photodegradation efficiency under sunlight was calculated for 1.5 h with eq. (1). Figure 11 shows the photodegradation of MB with TiO<sub>2</sub> NPs and compares it with photodegradation by the TiO<sub>2</sub>/PAAm hydrogel (containing 0.5% w/v TiO<sub>2</sub>). After 1.5 h, 95.40% of the dye was degraded. The rate of MB degradation with TiO<sub>2</sub>/PAAm was lower than that with

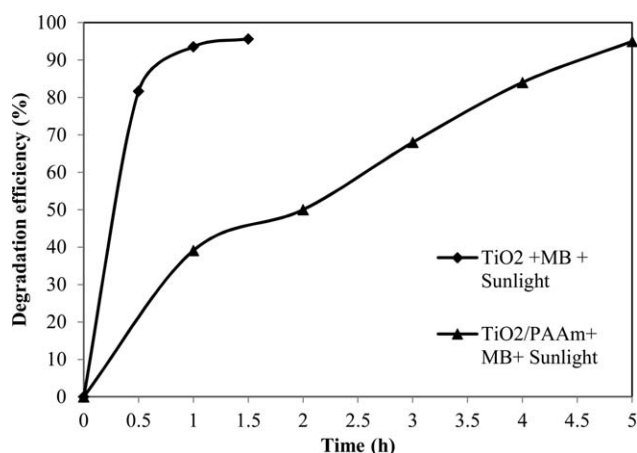


**Figure 11.** Photodegradation of MB with TiO<sub>2</sub> P25 powder without a hydrogel matrix.

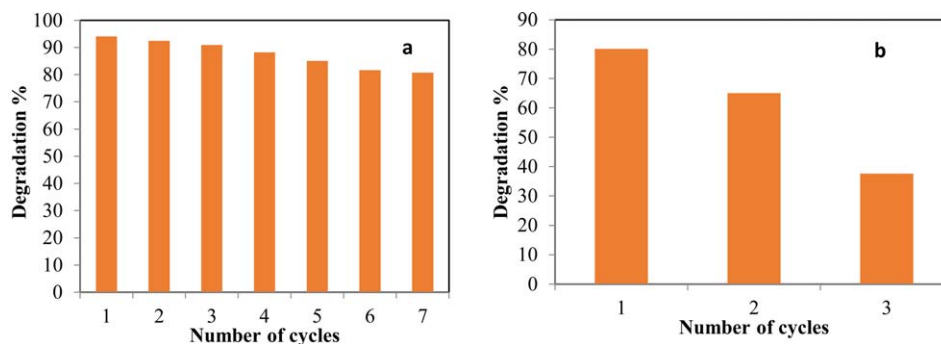


**Figure 12.** Photocatalytic degradation of MB with the (a) 0.5% w/v TiO<sub>2</sub>/PAAm photocatalyst and (b) TiO<sub>2</sub> P25 NPs after the indicated number of recycling times. [Color figure can be viewed in the online issue, which is available at [wileyonlinelibrary.com](http://wileyonlinelibrary.com).]

TiO<sub>2</sub> powder. Because in this case, TiO<sub>2</sub> NPs were trapped in the hydrogel matrix, and so, only TiO<sub>2</sub> NPs that were on the surface of the hydrogel could participate in dye degradation, and the surface areas of the active TiO<sub>2</sub> NPs decreased.

### Recycling of the Photocatalyst

The easy recycling and reusability of the photocatalyst are advantages of TiO<sub>2</sub> NPs immobilized in a hydrogel matrix that are important in practical applications.<sup>29</sup> The recycling of the TiO<sub>2</sub>/PAAm photocatalyst was carried out with a constant concentration of MB (10 ppm) and 0.2 g of photocatalyst in each cycle. After each cycle, TiO<sub>2</sub>/PAAm photocatalyst was collected, washed with distilled water, and dried, and the recovered photocatalyst was used for the next cycle. Figure 12(a) shows the number of recycling times. The degradation efficiency of the TiO<sub>2</sub>/PAAm photocatalyst decreased from 94.00% in the first cycle to 80.70% in the seventh cycle. These results indicate that the TiO<sub>2</sub>/PAAm photocatalyst served its efficiency because immobilizations of the TiO<sub>2</sub> NPs in the hydrogel matrix facilitated recycling and the TiO<sub>2</sub> NPs showed no weight loss. To confirm this result, the recycling experiment was carried out with TiO<sub>2</sub> NPs (6 mg) in the powdery state for the MB photodegradation of [10 ppm; Figure 12(b)]. During recycling and washing, the powdery TiO<sub>2</sub> NPs showed weight loss, and degradation decreased from 80.0% in the first cycle to 37.6% at the end of the third cycle.

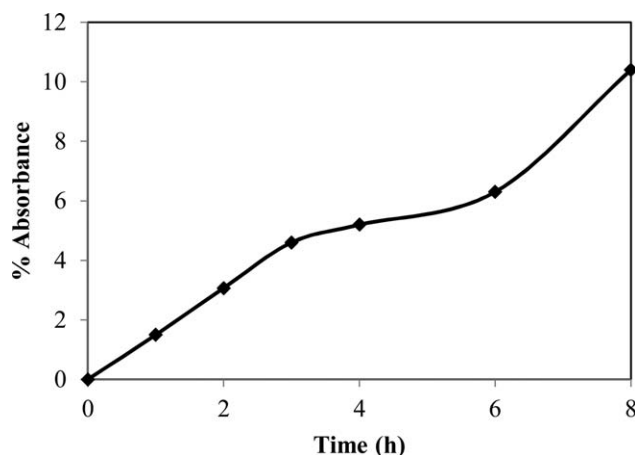


**Figure 13.** Degradation of MB in the dark.

### Effect of Light in MB Degradation

To confirm the role of light in MB degradation, the degradation of MB (10 ppm) by TiO<sub>2</sub>/PAAm (0.2 g) was carried out in the dark. Figure 13 shows the results after 8 h.

According to Figure 13, in the absence of light, only about 10% of MB was absorbed by TiO<sub>2</sub>/PAAm, and dye degradation did not occur. This result confirmed that MB degradation was a photocatalytic reaction, and light was a necessary factor.

### CONCLUSIONS

A TiO<sub>2</sub>/PAAm hydrogel was synthesized by TiO<sub>2</sub> P25 NPs as the initiator by photopolymerization from an aqueous solution. Structural investigations, including FTIR spectroscopy, SEM, and TEM images, confirmed the dispersion of TiO<sub>2</sub> NPs in the hydrogel. To investigate the photocatalytic activity of the TiO<sub>2</sub>/PAAm hydrogel, we applied the degradation of MB. The results show that about 95.00% of a 10 mg/L MB solution was photocatalytically degraded after 5 h under sunlight irradiation. The TiO<sub>2</sub>/PAAm hydrogel was recycled easily seven times without a significant decrease in the degradation efficiency (94.00% in first recycle and 80.70% at the end of seven recycle). Also, the results of MB degradation in the dark confirmed that this process was a photocatalytic reaction and the presence of light was necessary. So, we hoped that this hydrogel could be used to degrade organic pollutants.

This study had several advantages compared to other similar studies: the degradation process was carried out in one step under sunlight, whereas in other studies, such as those of Kangwansupamonkon *et al.*<sup>15</sup> and Zhang *et al.*,<sup>21</sup> degradation was done in two steps, first, the absorption of MB into the hydrogel and, second, dye removal from the colored hydrogel under UV light.

Other advantage of this study included the use of TiO<sub>2</sub> NPs as an initiator instead of harmful chemical initiators. TiO<sub>2</sub> had two important roles, as an initiator and a degradation agent; this caused this method to be ecofriendly and cost effective. However, in many previously reported study, TiO<sub>2</sub> had only a degradation role, and the initiators were other chemicals. Also, in this study, the number of recycling times of the synthesized hydrogel was greater than those of other reported works.



## REFERENCES

1. Busch, G. *Eur. J. Phys.* **1989**, *10*, 254.
2. Hoffmann, M. R.; Martin, S. T.; Choi, W.; Bahnemann, D. W. *Chem. Rev.* **1995**, *95*, 69.
3. Khataee, A. R.; Kasiri, M. B. *J. Mol. Catal. A* **2010**, *328*, 8.
4. Robinson, T.; McMullan, G.; Marchant, R.; Nigam, P. *Biore-sour. Technol.* **2001**, *77*, 47.
5. Sills, M. R.; Zinkham, W. H. *Arch. Pediatr. Adolesc. Med.* **1994**, *148*, 306.
6. Crini, G. *Prog. Polym. Sci.* **2005**, *30*, 38.
7. Crittenden, J. C.; Zhang, Y.; Hand, D. W.; Perram, D. L.; Marchand, E. G. *Water Environ. Res.* **1996**, *68*, 270.
8. Behnajady, M. A.; Modirshahla, N. *Chemosphere* **2006**, *62*, 1543.
9. Wang, H.-L.; Liu, L.-Y.; Kou, W.-Q.; Jiang, W.-F. *J. Polym. Compos.* **2013**, *34*, 681.
10. Khataee, A. R.; Pons, M. N. *J. Hazard. Mater.* **2009**, *168*, 451.
11. Mital, G. S.; Manoj, T. *Chin. Sci. Bull.* **2011**, *56*, 1639.
12. Zand, Z.; Kazemi, F.; Hosseini, S. *Tetrahedron Lett.* **2014**, *55*, 338.
13. Santos, D. T.; Sarrouh, B. F.; Rivaldia, J. D.; Converti, A.; Silva, S. S. *J. Food Eng.* **2008**, *86*, 542.
14. Eskandari, P.; Kazemi, F.; Azizian-Kalandaragh, Y. *Sep. Purif. Technol.* **2013**, *120*, 180.
15. Kangwansupamonkon, W.; Jitbunpot, W.; Kiatkamjornwong, S. *Polym. Degrad. Stab.* **2010**, *95*, 1894.
16. Jamal, R.; Osman, Y.; Rahman, A.; Ali, A.; Zhang, Y.; Abdiryim, T. *Mater.* **2014**, *7*, 3786.
17. Manohar, R. P.; Shrivastava, V. S. *Der Chem. Sinica* **2014**, *5*, 8.
18. Jiang, W.; Liu, Y.; Wang, J.; Zhang, M.; Luo, W.; Zhu, Y. *Adv. Mater. Interfaces* **2015**, to appear.
19. Mohamadnia, Z.; Jamshidi, A.; Mobedi, H.; Ahmadi, E.; Zohuriaan-Mehr, M. J. *Iran. Polym. J.* **2007**, *16*, 711.
20. Popovi, I. G.; Katsikas, L.; Weller, H. *Polym. Bull.* **1994**, *32*, 597.
21. Zhang, D.; Yang, J.; Bao, S.; Wu, Q.; Wang, Q. *Sci. Rep.* **2013**, *3*, 1.
22. Ni, X. Y.; Ye, J.; Dong, C. *J. Photochem. Photobiol. A* **2006**, *181*, 19.
23. Huang, Z. Y.; Barber, T.; Mills, G.; Morris, M. B. *J. Phys. Chem.* **1994**, *98*, 12746.
24. Nakashima, T.; Sakashita, M.; Nonoguchi, Y.; Kawai, T. *Macromol.* **2007**, *40*, 6540.
25. Stroyuk, A. L.; Granchak, V. M.; Korzhak, A. V.; Ya Kuchmii, S. *J. Photochem. Photobiol. A* **2004**, *162*, 339.
26. Bao, S.; Wu, D.; Wang, Q.; Su, T. *PLoS One* **2014**, *9*, 1.
27. Okay, O.; Oppermann, W. *Macromolecules* **2007**, *40*, 3378.
28. Marija, L.; Nedeljko, M.; Maja, R.; Zoran, S.; Marija, R.; Melina, K. K. *Polym. Compos.* **2014**, *35*, 806.
29. Jagadish, N. H.; Vishalakshi, B. *Der. Pharm. Chem.* **2012**, *4*, 946.
30. Muralimohan, Y.; Sudhakar, K.; Kesavamurthy, P. S.; Mohanraju, K. *Int. J. Polym. Mater.* **2006**, *55*, 513.
31. Chirila, T. V.; Constable, I. J.; Crawford, G. J.; Vijayasekaran, S.; Thompson, D. E.; Chen, Y. C.; Fletcher, W. A.; Griffin, B. *J. Biomater.* **1993**, *14*, 26.
32. Tang, Q.; Lin, J.; Wu, Z. *Eur. Polym. J.* **2007**, *43*, 2214.
33. Gajbhiye, S. B. *IJMERE* **2012**, *2*, 1204.
34. Fang-Bai, L.; Guo-Bang, G.; Guo-Feng, H.; Yun-Li, G.; Hong-Fu, W. *J. Inv. Sci.* **2001**, *13*, 64.
35. Wang, X.; Mei, L.; Xing, X.; Liao, L.; Lv, G.; Li, Z.; Wu, L. *Appl. Catal. B* **2014**, *160–161*, 211.
36. Harikumar, P. S.; Joseph, L.; Dhanya, A. *J. Environ. Eng. Ecol. Sci.* **2013**, *2*, 1.
37. Kaur, J.; Bansal, S.; Singhal, S. *Phys. B* **2013**, *416*, 33.
38. Lee, J.; Nam, W.; Kang, M.; Yoon, K.; Kim, M.; Ogino, K.; Miyata, S.; Choung, S. *Appl. Catal. A* **2003**, *244*, 49.
39. Toor, A.; Verma, A.; Jotshi, C.; Bajpai, P.; Singh, V. *Dyes Pigments* **2006**, *68*, 53.